NASA/CR-2002-212135
ICASE Report No. 2002-47

Wholly Aromatic Ether-imides. Potential Materials for *n*-Type Semiconductors

Theo J. Dingemans
ICASE, Hampton, Virginia

Terry L. St Clair
NASA Langley Research Center, Hampton, Virginia

Edward T. Samulski
University of North Carolina at Chapel Hill, Chapel Hill, North Carolina

December 2002

The NASA STI Program Office . . . in Profile

Since its founding, NASA has been dedicated to the advancement of aeronautics and space science. The NASA Scientific and Technical Information (STI) Program Office plays a key part in helping NASA maintain this important role.

The NASA STI Program Office is operated by Langley Research Center, the lead center for NASA's scientific and technical information. The NASA STI Program Office provides access to the NASA STI Database, the largest collection of aeronautical and space science STI in the world. The Program Office is also NASA's institutional mechanism for disseminating the results of its research and development activities. These results are published by NASA in the NASA STI Report Series, which includes the following report types:

- TECHNICAL PUBLICATION. Reports of completed research or a major significant phase of research that present the results of NASA programs and include extensive data or theoretical analysis. Includes compilations of significant scientific and technical data and information deemed to be of continuing reference value. NASA's counterpart of peer-reviewed formal professional papers, but having less stringent limitations on manuscript length and extent of graphic presentations.

- TECHNICAL MEMORANDUM. Scientific and technical findings that are preliminary or of specialized interest, e.g., quick release reports, working papers, and bibliographies that contain minimal annotation. Does not contain extensive analysis.

- CONTRACTOR REPORT. Scientific and technical findings by NASA-sponsored contractors and grantees.

- CONFERENCE PUBLICATIONS. Collected papers from scientific and technical conferences, symposia, seminars, or other meetings sponsored or cosponsored by NASA.

- SPECIAL PUBLICATION. Scientific, technical, or historical information from NASA programs, projects, and missions, often concerned with subjects having substantial public interest.

- TECHNICAL TRANSLATION. English-language translations of foreign scientific and technical material pertinent to NASA's mission.

Specialized services that complement the STI Program Office's diverse offerings include creating custom thesauri, building customized data bases, organizing and publishing research results . . . even providing videos.

For more information about the NASA STI Program Office, see the following:

- Access the NASA STI Program Home Page at ***http://www.sti.nasa.gov***

- Email your question via the Internet to help@sti.nasa.gov

- Fax your question to the NASA STI Help Desk at (301) 621-0134

- Telephone the NASA STI Help Desk at (301) 621-0390

- Write to:
  NASA STI Help Desk
  NASA Center for AeroSpace Information
  7121 Standard Drive
  Hanover, MD 21076-1320

NASA/CR-2002-212135
ICASE Report No. 2002-47

Wholly Aromatic Ether-imides. Potential Materials for *n*-Type Semiconductors

Theo J. Dingemans
ICASE, Hampton, Virginia

Terry L. St Clair
NASA Langley Research Center, Hampton, Virginia

Edward T. Samulski
University of North Carolina at Chapel Hill, Chapel Hill, North Carolina

ICASE
NASA Langley Research Center
Hampton, Virginia
Operated by Universities Space Research Association

Prepared for Langley Research Center
under Contract NAS1-97046

December 2002

Available from the following:

NASA Center for AeroSpace Information (CASI)
7121 Standard Drive
Hanover, MD 21076-1320
(301) 621-0390

National Technical Information Service (NTIS)
5285 Port Royal Road
Springfield, VA 22161-2171
(703) 487-4650

WHOLLY AROMATIC ETHER-IMIDES. POTENTIAL MATERIALS FOR *n*-TYPE SEMICONDUCTORS

THEO J. DINGEMANS[*], TERRY L. ST CLAIR[§] AND EDWARD T. SAMULSKI[‡]

Abstract. We report on the synthesis and characterization of a novel series low-molar-mass ether-imide rod-shaped model compounds. All ether-imides were obtained by terminating the appropriate rigid core dianhydride, *i.e*. pyromellitic dianhydride (**PMDA**), 1,4,5,8-naphthalenetetracarboxylic dianhydride (**NDA**), 3,3',4,4'-biphenyltetracarboxylic dianhydride (**BPDA**), and 3,3',4,4'-oxydiphthalic dianhydride (**ODPA**) with three flexible aryl-ether tails of different chain length. The mono-functional aryl-ether amines, *i.e*. 4-(3-phenoxy-phenoxy)-phenylamine (**2**) and 4-(3-phenoxy-3-phenoxy-phenoxy)-phenylamine (**4**), were synthesized using standard fluoro-displacement and Ullmann condensation techniques. The corresponding ether-imide model compounds were obtained in high yields using a one-step solution imidization procedure. Increasing the number of *meta*-substituted aryl-ether units reduces the melt transition temperatures and at the same time it increases the solubility of the model compounds. Most model compounds are crystalline solids and form isotropic melts upon heating. 2,7-Bis-(-4-phenoxy-phenyl)-benzo[*lmn*][3,8]phenanthroline-1,3,6,8-tetraone (**NDA-n$_0$**), however, displays a smectic A (S_A) when cooled from the isotropic phase, followed by what appears to be either a highly ordered smectic phase or a columnar phase. This is the first example, known to date, in which a mesophase is detected in a wholly aromatic ether-imide compound. For all compounds we present spectroscopic data and X-ray diffraction data. Cyclic voltammetry was used to determine the redox behavior and pertinent energy levels of the model compounds.

Key words. ether-imide, liquid crystal, organic semiconductor

Subject classification. Structures and Materials

1. Introduction. Poly(ether-imide)s (PEIs) are a well-known class of engineering plastics with outstanding mechanical properties, high thermal stability and excellent chemical resistance towards a wide range of solvents.[1, 2] PEI films are used extensively in a variety of electronic applications, *i.e.* insulating layers, circuit boards and low dielectric coatings.[2] In recent years, new applications for wholly aromatic ether-imides have emerged. Several groups have demonstrated that PEIs with naphthalene and perylene moieties can be used as electrochromic polymers, which some day may find use in variable reflectance mirrors [3] and organic light emitting diodes (OLEDs).[4] More recently, Katz and co-workers demonstrated that low-molecular-weight imides can be used in organic *n*-type semiconductor devices such as field-effect transistors (FETs) and Schottky diodes. [5] Their naphthalene based compounds with terminal fluorinated tails show high electron mobilities (> 0.1 $cm^2V^{-1}s^{-1}$) and excellent on/off current ratios ($>10^5$), even in the presence of air. Previously, devices based *n*-type organic materials failed because the presence of oxygen limited the lifetime of these devices. The close molecular packing in the fluorinated imides synthesized by the Katz group, however, is believed to prevent oxygen and moisture permeation and improve device lifetime and performance.

Based on these promising results, we believe that wholly aromatic imide-based liquid crystals would provide several advantages over non-mesogenic compounds. Liquid crystals are well known for their outstanding barrier properties, and when designed properly, their unique packing motives could result in improved charge-carrier mobilities.[5] Conceivably, rigid aromatic dianhydrides terminated with an appropriate aryl-ether amine could posses these useful liquid crystalline properties. Although some groups have reported on low-molecular-weight imide based liquid crystals [6, 7], these compounds

*Author for correspondence. ICASE, Mail Stop 132C, NASA Langley Research Center, Hampton, VA 23681-2199 (email: t.j.dingemans@larc.nasa.gov). This research was supported by the National Aeronautics and Space Administration under Contract No. NAS1-97046 while the author was in residence at ICASE, NASA Langley Research Center, Hampton, VA 23681-2199.
‡ Department of Chemistry, University of North Carolina at Chapel Hill, Chapel Hill, NC 27599-3290.
§ Advanced Materials and Processing Branch, NASA Langley Research Center, Hampton, VA 23681-2199.

contain aliphatic units which lack the oxidative stability necessary for semiconductor applications. In order to address this problem, we recently published our results on a series of soluble low-molecular-weight imides with terminal fluorinated tails [8], but to date, no wholly aromatic polymeric or low molecular weight ether-imide liquid crystals have been reported in the literature.

To this end, we report the synthesis and characterization of a series ether-imide model compounds, with the classic calamitic "tail-core-tail" structure.[9] As shown in Figure 1, we have terminated four dianhydrides, *i.e*. pyromellitic dianhydride (**PMDA**), 1,4,5,8-naphthalene-tetracarboxylic dianhydride (**NDA**), 3,3',4,4'-biphenyltetracarboxylic dianhydride (**BPDA**), and 3,3',4,4'-oxydiphthalic dianhydride (**ODPA**), with a homologous series *meta*-substituted aryl-ether amines to study the melt behavior, phase type, solubility and electronic properties of these compounds.

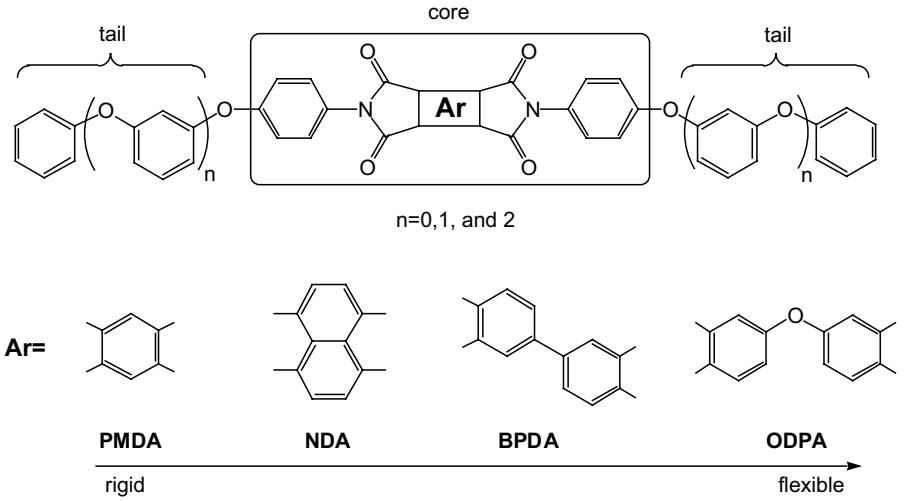

FIG 1. *Ether-imide model compounds.* ***PMDA****= pyromellitic dianhydride,* ***NDA****=1,4,5,8-Naphthalenetetracarboxylic dianhydride,* ***BPDA****= 3,3',4,4'-biphenyltetracarboxylic dianhydride,* ***ODPA****= 3,3',4,4'-oxydiphthalic dianhydride.*

We designed the wholly aromatic aryl-ether amines, 4-phenoxy-phenylamine (n=0), 4-(3-phenoxy-phenoxy)-phenylamine (n=1), and 4-(3-phenoxy-3-phenoxy-phenoxy)-phenylamine (n=2) with the following rational in mind. The terminal *p*-phenylamine functionality initially increases the aspect ratio of the resulting di-imide rigid core, while the bulky *meta*-substituted aryl-ether flexible units would provide the flexible tail. Also, the latter will reduce the melt transition of the high-melting di-imide rigid core and stabilize the molecular orientations necessary for mesophase formation. Aryl-ether flexible tails have not been used previously as flexible tail segments in liquid crystals, and compared to typical alkyl or alkyloxy flexible tails, aryl-ether tails have more breath, which keeps the overall diameter of the mesogens more uniform.

2. Results and Discussion. Both flexible aryl-ether amines were easy to prepare in acceptable overall yields. All model compounds were conveniently synthesized in one step. All ether-imides with n= 0 were reported before, and were used as monomers towards aromatic ether-ketone polymers [10, 11] or as model compounds for spectroscopic molecular modeling studies.[12-15] Compounds reported in this study, where n=1 or 2, are believed to be new compounds. We found that all **PMDA**-based ether-imides (with n= 0,1, and 2) showed limited solubility in common chlorinated solvents (CH_2Cl_2 and $CHCl_3$), but appear soluble in hot DMSO and 1,2-dichlorobenzene. All **NDA**-, **BPDA**- and **ODPA**-based compounds (with n= 0,1, and 2) show excellent solubilities in THF, CH_2Cl_2 and $CHCl_3$. All model compounds, with the exception of the **ODPA**-series, have a yellow appearance, indicative of conjugated aromatic π-π* systems. The oxygen atom in 3,3',4,4'-oxydiphthalic dianhydride disrupts the conjugation between the adjacent phenyl rings and this results in colorless compounds.

2.1. Thermal Properties. The phase behavior and DSC results of the pyromellitic dianhydride (**PMDA**), 1,4,5,8-naphthalenetetracarboxylic dianhydride (**NDA**), 3,3',4,4'-biphenyltetracarboxylic dianhydride (**BPDA**), and 3,3',4,4'-oxydiphthalic dianhydride (**ODPA**)-based model compounds are summarized in Appendix 1. The phase and melt behavior of all model compounds are displayed in Figure 2. Each bar diagram shows three pairs of columns. The left column of each pair represents the heating scan, whereas the right column represents the cooling scan.

From Figure 2 it is evident that the *meta*-substituted aryl-ether flexible tails are very effective in disrupting the delicate intra-molecular packing within these compounds. As the number of aryl-ether units increases, a significant reduction in melt transition is observed for all compounds. The **PMDA**- and **NDA**-based compounds, as shown in Figure 2a and 2b, are least affected by the aryl-ether modifications. Overall, the trend is a reduction of the melt-transition temperature but upon cooling from the isotropic, or the anisotropic phase, the molecules are able to pack into a crystal lattice almost immediately.

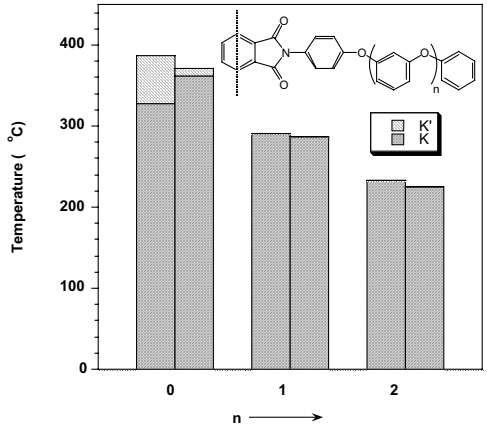

FIG. 2a. *Melt behavior of the **PMDA**-based model (**K** and **K'** denote different crystal phases)*

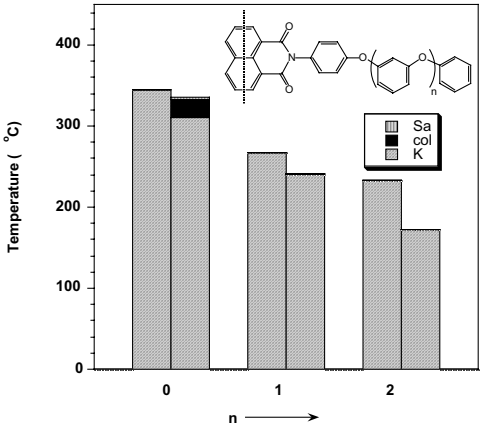

FIG. 2b. *Melt behavior of the **NDA**-based model compounds* compounds *(**S**$_x$ denotes unknown smectic and **S**$_A$ smectic-A)*

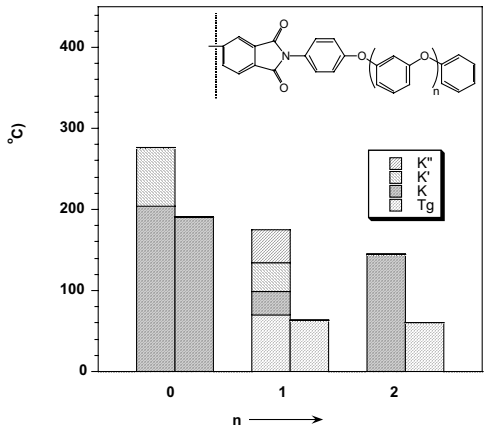

FIG. 2c. *Melt behavior of the **BPDA**-based model compounds (**K**, **K'**, and **K''** denote different crystal phases and Tg =glass transition temperature, respectively)*

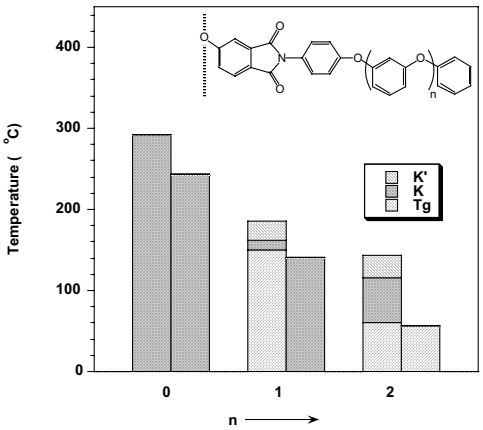

FIG. 2d. *Melt behavior of the **ODPA**-based model compounds (**K** and **K'** denote different crystal phases and Tg =glass transition temperature, respectively)*

The **BPDA**- and **ODPA**-based compounds, shown in Figure 2c and 2d, display moderate to severe super cooling behavior. Both **BPDA**- and **ODPA**-based ether-imides, where n=1 or 2, show softening points, or glass-transition temperatures, when n=1 and 2. The compounds can be quenched into an amorphous glass from the isotropic melt. Figure 3 shows the DSC trace for **BDPA-n$_1$** and this scan is representative for the **BPDA**- and **ODPA**-series where n=1 and 2. Upon heating a second order phase transition, i.e. a shift in baseline, is observed at 65 ^{o}C, which is indicative for the glass-transition temperature or T_g.

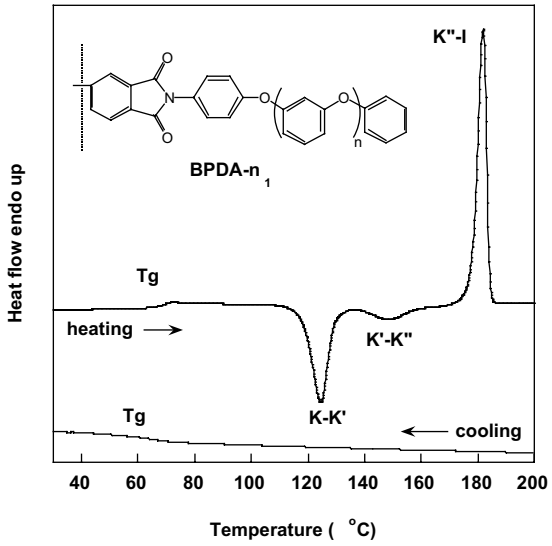

FIG 3. *DSC heating and cooling trace of* ***BPDA-n$_1$***

When heating is continued two crystal to crystal transition can be seen at 130 ^{o}C (K-K') and 150 ^{o}C (K'-K"), followed by the melt transition at 180 ^{o}C (K"-I). Cooling from the isotropic melt results in an amorphous glass with a T_g at 63 ^{o}C.

2.2. Mesophase Behavior. Although the **PMDA-**, **NDA-** and **BPDA**-based compounds have distinct features, that would promote mesophase formation, we found that only one model compound appeared to be mesogenic. Even more surprising is the fact that **NDA-n$_0$**, rather than **PMDA-n$_0$** or **BPDA-n$_0$**, melts into a mesophase. Eiselt *et al*. [7] showed that **BPDA** is an excellent mesogenic core when terminated with a variety of alkyl- or alkyloxy-phenylamines. **PMDA**, on the other hand, has been reported to form mesophases but these compounds are often too high melting (>400 ^{o}C), and are only melt-processable when a high concentration of long alkyloxy chains are used.[16] Although the synthesis of 2,7-bis-(-4-phenoxy-phenyl)-benzo[*lmn*] [3,8]phenanthroline-1,3,6,8-tetraone (**NDA-n$_0$**) has been reported before [10], the authors did not report mesophase behavior for this compound. Using 1,4,5,8-naphthalene (**NDA**) as the rigid core moiety introduces several subtle changes with respect to the overall molecular shape and electrostatics of the model compounds. The shape of the rigid core widens –and hence lowers the aspect ratio– which usually destabilizes mesophase formation.[9] Instead of linking the flexible aryl-ether tails through a five-membered anhydride, a six-membered anhydride is formed. The latter is expected to have improved conjugation through the 4-membered di-imide core as demonstrated by Havens *et al*.[15], and is believed to have a stabilizing effect on mesophase formation.[17] Figure 4 shows a DSC heating and cooling scan of 2,7-bis-(-4-phenoxy-phenyl)-benzo[*lmn*][3,8]phenanthroline-1,3,6,8-tetraone (**NDA-n$_0$**).

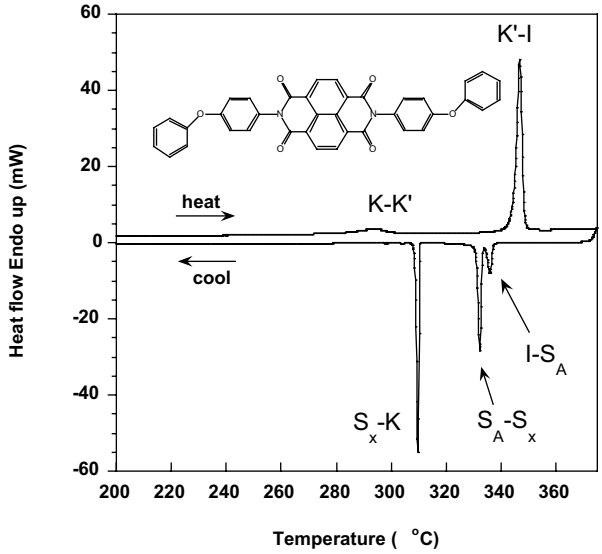

FIG 4. *Second heating and cooling trace of 2,7-bis-(-4-phenoxy-phenyl)-benzo[lmn][3,8]phenanthroline-1,3,6,8-tetraone* ***(NDA-n$_0$)****. The heating scan shows a crystal to crystal transition (K-K') and the crystal to isotropic transition (K'-I); the cooling scan shows three transitions which correspond to the isotopic to smectic A (I-S_A), smectic A to smectic X (S_A-S_X) and S_X to crystal (S_X-K) transitions, respectively.*

2.3. Optical Microscopy Results. The melt behavior of all compounds was investigated using a polarizing optical microscope. Although the model compounds can be viewed as classic "tail-core-tail' mesogens, we only observed mesomorphism in **NDA-n$_0$**. The textures of **NDA-n$_0$** are summarized in Figure 5.

The phase behavior for **NDA-n$_0$** is monotropic, *i.e.* mesomorphism was observed upon cooling only. Figure 5a shows the formation of smectic A (S_A) batonnets at 334 ^oC when **NDA-n$_0$** was slowly cooled (5 $^oC.min^{-1}$) from the isotropic phase. This texture evolved rapidly into a typical smectic A (S_A) focal conic texture, shown in Figure 5b, and this phase is only stable over a 3^o temperature range. When cooling was continued, the focal conic texture transformed into an unusual fern-like texture, which we believe, could be indicative of a columnar mesophase.[18] Figure 5c shows this transition at 333 ^oC where the S_A phase almost immediately transformed into the columnar phase.

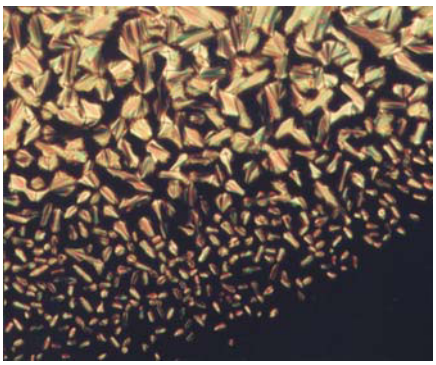

FIG. 5a. ***NDA-n$_0$*** *at 335 ^oC. Formation of batonnets upon; cooling from the isotropic phase; crossed polars and 20X.*

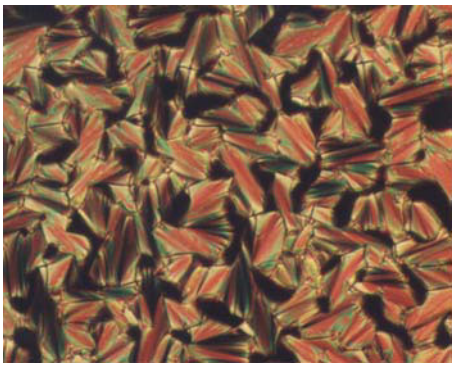

FIG. 5b. ***NDA-n$_0$*** *at 334 ^oC. Fully developed focal conic fans (S_A); crossed polars and 20X.*

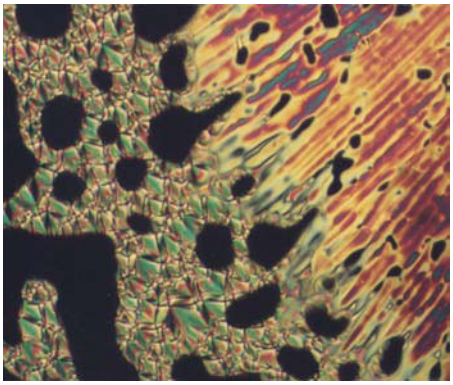

FIG. 5c. ***NDA-n$_0$*** *at 333 °C. S_A phase (left) co-existing with the smectic X (S_X); crossed polars and 20X.*

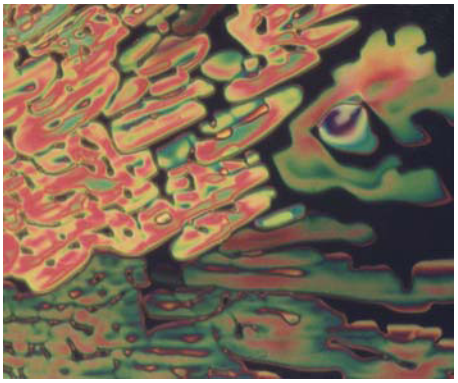

FIG. 5d. ***NDA-n$_0$*** *at 330 °C. S_X phase; crossed polars and 20X.*

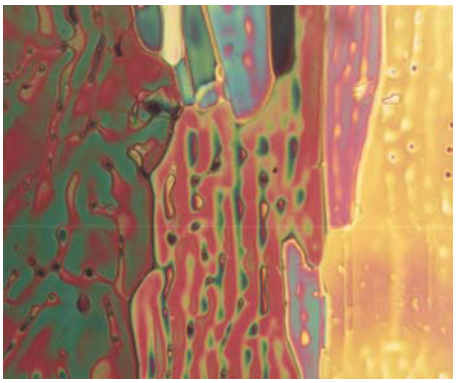

FIG. 5e. ***NDA-n$_0$*** *at 320 °C. Fully developed fern-like texture of the S_X phase; crossed polars and 20X.*

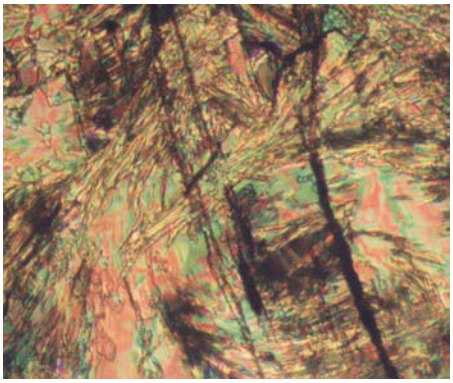

FIG. 5f. ***NDA-n$_0$*** *at 310 °C. Crystal phase (K); crossed polars and 20X.*

When the S_A phase was cooled very slowly (2 °C.min^{-1}) a homeotropic aligned phase could be observed from which the columnar texture emerges, this event is shown in Figure 5d. The fully developed fern texture at 320 °C is shown in Figure 5f, and finally, Figure 5f shows the texture for the crystalline phase (K) of **NDA-n$_0$** at 310 °C.

2.4. X-Ray Diffraction Results. In order to gain more insight into the phase behavior of **NDA-n$_0$**, we performed temperature-dependent X-ray diffraction experiments on an unaligned sample. **NDA-n$_0$** was heated into the isotropic phase and slowly cooled (2 °C/min) into the S_A phase. Unfortunately, we were not able to determine the layer spacing of the S_A phase because the small temperature window of this phase prevented us from taking any measurements. When cooling was continued into the S_X, however, we observed an X-ray diffractogram as shown in Figure 6. The pattern consists of a broad diffuse halo in the wide-angle region at ~ 5.1 Å, and is indicative of the liquid-like order of this phase. In the small angle region we observe one sharp reflection and one shoulder which correspond to *d*-spacings of 26.6 and 20.9 Å respectively. It appears that the intermolecular correlation in this mesophase is rather large, which is typical observed for columnar phases where the mesogens show a large degree of disorder in the columns. The DSC data, however, shows a smectic A (S_A) to smectic X (S_X) enthalpy of 24.7 kJ.mol^{-1}, which is large, and would be more consistent with a highly ordered mesophase. We believe that the strong intermolecular interactions between the polar naphthalene di-imide cores and the absence of flexible aliphatic tails are responsible for this high enthalpic value.

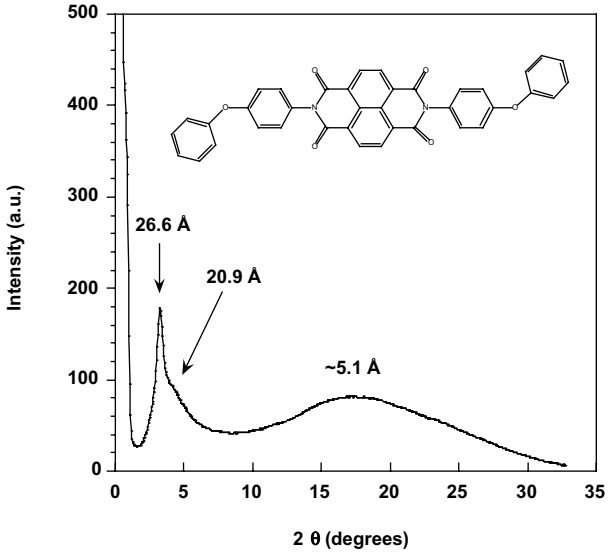

FIG. 6. *Powder X-ray diffraction pattern of* ***NDA-n$_0$*** *at 320 ^oC*

Currently, however, we are not able to positively identify this mesophase and we are attempting to obtain additional information from X-ray using magnetically aligned samples of **NDA-n$_0$**. To the authors' knowledge, **NDA-n$_0$** is the first example of a wholly aromatic liquid crystal ether-imide. In addition, the overall molecular shape of this compound is more ellipsoid rather than disk-shaped, which make the observation of a columnar mesophase even more remarkable. We also note that we don't know of any other mesogens that form columnar mesophases wherein only two peripheral units are present and flexible aliphatic tails are absent.

2.5. Single Crystal X-Ray Diffraction Results. We used single crystal X-ray structure determinations in order to gain more detailed information about the molecular shape of our mesogenic **NDA-n$_0$** model compound, and to infer potential molecular packing motifs in the liquid crystal phases. Figure 7 shows a perspective view of the molecular packing of **NDA-n$_0$** along the *a* and *c* axis.

The diffraction pattern in the crystalline phase could be indexed on an monoclinic unit cell of dimensions a = 7.5736 Å, b = 5.2290 Å, and c = 35.678 Å (detailed crystal and structure refinement data are summarized in Appendix 2) and the molecular length in this configuration was found to be 26.038 Å. The distance between adjacent planar naphthalene cores is 5 Å, and this appears to be consistent with the intermolecular distance we observed in the liquid crystal phase. Although the steric interaction between the phenyl ring and the six-membered imide ring is high, a planar conformation seems to be the preferred packing.

Katz *et al*. reported high electron mobilities (> 0.1 $cm^2V^{-1}s^{-1}$) and on/off current ratios (> 10^5) for a similar **NDA** based compound but with fluorinated tails.[5] In their case, however, the molecules preferred a herringbone packing motif while we observe a packing where the naphthalene di-imide cores adopt a co-planar packing. The latter, we believe, will promote π-overlap between adjacent molecules and the combination of high stability in air and high solubility in common solvent make these ether-imide model compounds interesting candidates for *n*-type semiconductors.[4]

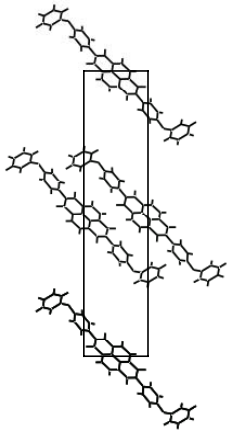

FIG. 7. A-*Crystal packing diagram of* ***NDA-n$_0$****. The unit cell parameters are a = 7.5736 Å, b = 5.2290 Å, and c = 35.678 Å, β= 91.251 º and Z=2.*

2.6. Spectroscopic measurements. Dilute solutions (c= 1 mg/L) of all compounds in dichloromethane (CH_2Cl_2) were investigated using UV/Vis spectroscopy. Figure 8 summarizes the absorption spectra of all model compounds, *i.e.* **PMDA**, **NDA**, **BPDA**, and **ODPA** where n= 0,1, and 2.

In order to gain more insight into the electronic properties of polyether-imides (PEIs) and their low-molecular weight counterparts, we investigated all compounds using UV-Vis spectroscopy. The UV-Vis spectrum of **PMDA-n$_0$**, shown in Figure 8, is largely consistent with results published by Ishida *et.al*. [13]. This group reported absorption maxima of 310, 328, and 371 nm for this compound in trimethyl phosphate, while we observe absorption maxima at 279, 330 and 372 nm in dichloromethane. The fact that **PMDA-n$_0$** shows an absorption peak at 279 nm in dichloromethane (μ=1.6 D) as compared to 310 nm in the more polar trimethyl phospate (μ=2.8 D) constitutes a red shift, and is indicative of a π-π* transition.[19] Within the **PMDA** series we do not observe a relationship between absorption intensity and the length of the aryl-ether terminal tail.

The UV-Vis absorption spectra of the **NDA** series are summarized in Figure 8. The first absorption peak at λ_1= 272 nm is observed for all three compounds, and can be attributed to a π-π* transition, and in this case appears mainly associated with the aryl-ether flexible tails. When the number of aryl-ether units in the molecule increases, *i.e*. from n =0, 1, and 2, the relative intensity of this peak increases accordingly. The next set of peak maxima, 323, 340, 359, and 379 nm, can be attributed to the π-π* or n-π* transitions in the naphthalene-tetracarboxylic di-imide conjugated core. The transitions are well resolved and the location and intensity of the four peaks are independent of the length of the aryl-ether flexible tail, which confirms the fact that there is no electronic coupling between the naphthalene core and the *meta*-substituted aryl-ether tails.

The **BPDA** and **ODPA** ether-imides exhibit broad absorption peaks between 250 and 400 nm. The shoulders at 272 and 278 nm again are believed to be due to a π-π* transition. In case of the rigid compounds, *i.e*. **NDA** and **PMDA**, the transitions appear more well defined and show a clear maximum around 272 nm. When anhydrides were used that have a larger degree of flexibility, as is the case for the **BPDA** and **ODPA** based compounds, the conjugation length of the rigid core is interrupted and this results in broad, unresolved absorption peaks.

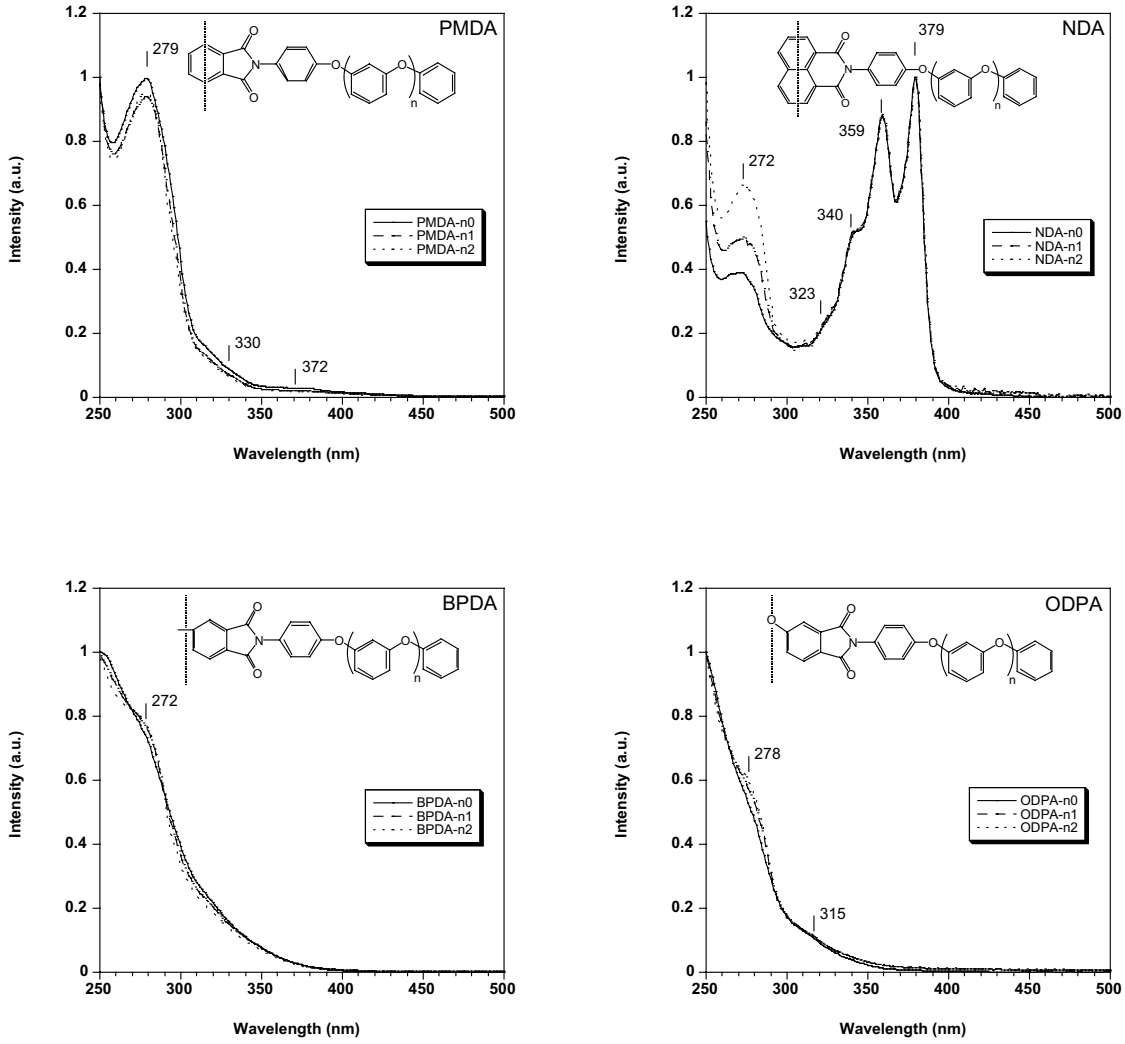

FIG. 8. *UV-Vis absorption spectra of the **PMDA, NDA, BPDA, and ODPA** model compounds (n= 0, 1, and 2) in dichloromethane (CH_2Cl_2) at ambient temperature.*

2.7. Cyclic voltammmetry. In order to study the electrochemical properties and determine the LUMO levels of the ether-imide model compounds, we investigated dilute solutions of the model compounds in deoxygenated tetrahydrofuran (THF) and tetrabutylammoniumhexafluorophosphate ($TBAPF_6$) as a supporting electrolyte. The results are summarized in Table 1.

From the four series only the **NDA** and **BPDA** based compounds showed reversible electrochemical behavior and no electrochemical polymerization after repeated scans. Both series undergo two distinct reversible reductions, the first involves the reduction of the neutral compound to the bis-anion radical, and the second reduction corresponds to the formation of the tetra-anion radical species.[20] Typical voltammograms of **NDA-n_1** and **BPDA-n_1** in THF with ferrocene as internal standard are shown in Figure 9.

TABLE 1.
*Reduction potentials of **NDA** and **BPDA** based model compounds vs. Ag/AgCl in THF at 25 °C.*

Compound	$Ered_1$ vs. Ag/AgCl [V]	$Ered_2$ vs. Ag/AgCl [V]	Ered1 vs. FOC [V]	LUMO [eV]
NDA-n_0	-0.485	-0.996	-1.08	-3.72
NDA-n_1	-0.475	-0.971	-1.07	-3.73
NDA-n_2	-0.482	-0.990	-1.08	-3.72
BPDA-n_0	-1.125	-1.353	-1.72	-3.08
BPDA-n_1	-1.128	-1.346	-1.72	-3.08
BPDA-n_2	-1.125	-1.347	-1.73	-3.07

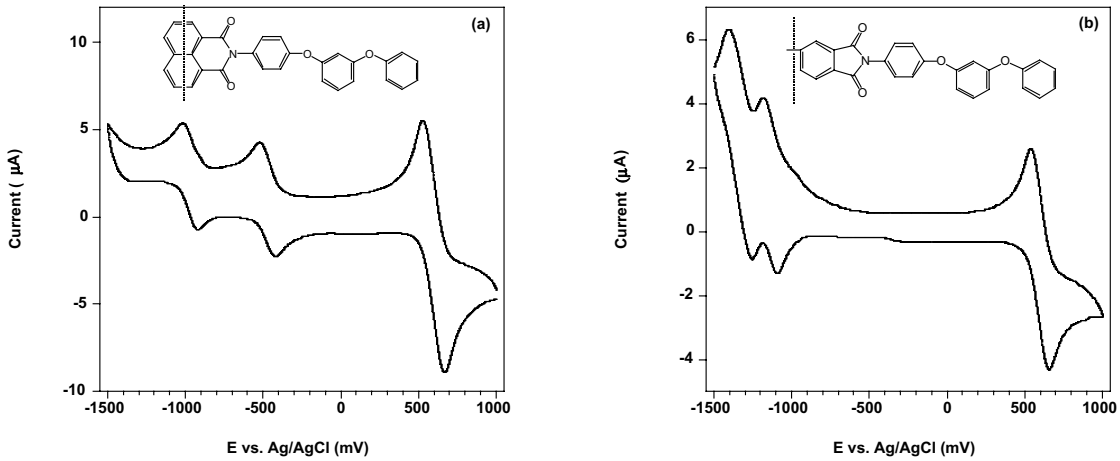

FIG. 9. *Typical cyclic voltammograms of **NDA-n_1** (a) and **BPDA-n_1** (b) with ferrocene in THF at room temperature. Scan rate: 100 mVs^{-1}.*

As expected, the length of the aryl-ether flexible tail does not affect the electrochemical properties of the ether-imides, rather they improve the solubility and hence their processability. All three **NDA** based compounds, with n= 0, 1, and 2, show similar reduction potentials ($Ered_1$ ~ -0.48 V and $Ered_2$ ~ -0.99 V vs. Ag/AgCl) and these data are in close agreement with values reported for other **NDA** based materials. [3, 20] The **BPDA** based compounds appear somewhat harder to reduce, as is reflected by their lower reduction potentials ($Ered_1$ ~ -1.13 V and $Ered_2$ ~ -1.35 V vs. Ag/AgCl).

The LUMO levels were calculated with reference to the energy level of ferrocene (-4.8 eV) according to well-known semi empirical methods.[21] The LUMO levels of the **NDA** based model compounds were calculated to be –3.72 eV while the LUMO levels of the **BPDA** based materials appear somewhat higher at –3.08 eV. These data suggest that both series are excellent electron transport materials and can be used in *n*-channel semiconductor devices.[4]

3. Concluding Remarks. We have investigated four different dianhydrides as the central core moiety of low-molecular weight ether-imides. The dianhydrides were terminated with 4-phenoxyaniline, 4-(3-phenoxy-phenoxy)-phenylamine, and 4-(3-phenoxy-3-phenoxy-phenoxy)-phenylamine. When the number of *meta*-substituted aryl-ether units increases, the melt-transition temperatures of all model compounds drop sharply as a consequence of weakened intermolecular packing interactions. When flexible dianhydrides were used, such as **BPDA** and **ODPA**, the melt behavior of the model compounds

became quite complex when the number of *meta*-substituted aryl-ether units in the flexible tail increased. These model compounds form amorphous glasses with well-defined glass-transition temperatures, and in addition, several crystalline phases were detected. Although the model compounds have typical mesogenic features, we found that all wholly aromatic ether-imide model compounds presented in this paper are poor mesogens. The only exception is **NDA-n$_0$**, which melts into a smectic A (S_A) and a unknown, possible smectic, mesophase. It appears that the molecular requirements for mesophase formation in **NDA-n$_0$** are very subtle and delicate. Although **NDA-n$_1$** does not melt into a mesophase (Figure 2a), we were initially hopeful that replacing the *meta*-substituted aryl ether for a *para*-substituted aryl ether would create a more linear mesogen (**I**) that would be more conducive to mesophase formation. This compound, however, melts into an isotropic phase at 367 ^oC and upon cooling crystallizes as 306 ^oC. Again, this confirms the fact that aryl-ethers disrupt the subtle intermolecular interaction that are required for mesophase formation, and therefore can not be used as flexible tails in low-molar-mass liquid crystals.

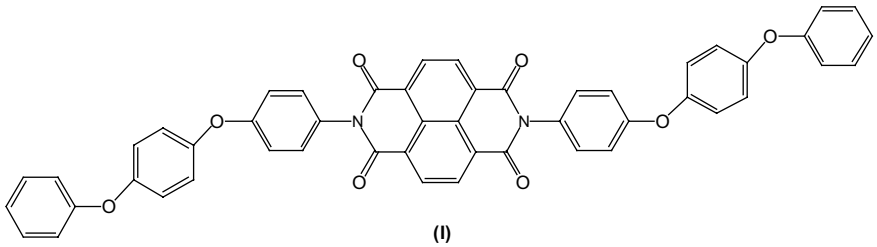

(I)

At present we are investigating the effects of different substitutions patterns on the 4-phenoxyaniline moiety and their effects on the phase behavior of **NDA-n$_0$**. We believe that the simplicity of **NDA-n$_0$** might improve our understanding of columnar mesophases with respect to which molecular factors influence phase stability and phase type. For this reason, we are pursuing single crystal X-ray diffraction experiments, to gain more insight in how these unusual ellipsoid mesogens pack into a crystal lattice, as well as temperature dependent X-ray diffraction experiments on oriented samples.

We are also exploring the possibility of using the **NDA**-based model compounds as *n*-type semiconductors for organic thin film photovoltaic, and molecular devices (*e.g.* FETs). Liquid crystalline *n*-type semiconductors build around a naphthalene rigid core could provide the high electron mobility, thermal stability and barrier properties required for producing high-quality thin film semiconductor devices.

4. Experimental.

4.1. Characterization. The structures of the intermediate and final products were confirmed using ^{1}H-NMR and ^{13}C-NMR spectroscopy. The spectra were recorded using a Bruker Avance 300 spectrometer (300 MHz and 75.46 MHz). Infrared spectra were collected using a Nicolet Magna-IR Spectrometer 750, and mass spectra (MS) were obtained using a Hewlett Packard 5972 spectrometer; M+ represents the molecular ion. UV-Vis absorption spectra were recorded with a Perkin-Elmer (Lambda9) Spectrometer.

Transition temperatures were determined using a Perkin Elmer Pyris differential scanning calorimeter (DSC), calibrated with indium (99.99%) (mp 156.5 ^oC, ΔH=28.315 J/g) and tin (99.99%) (mp 232.0 ^oC, ΔH=54.824 J/g). Heating and cooling scans were recorded at 10 °C/min. The melt behavior of the model compounds was studied using an Olympus BH-2 optical microscope, equipped with a Mettler Toledo FP82H hot stage. Samples were examined between untreated glass microscope slides.

Temperature dependant X-ray diffraction analysis (XRD) was carried out with an Enraf Nonius FR 590 system equipped with a two-dimensional image plate detector (2500 x 2500) pixels, 80 μm resolution. Unaligned samples were analyzed using monochromatic Cu-K_α (λ = 1.54 Å, 40 kV, 30 mA) radiation at various temperatures. The temperature was controlled with a Mettler Toledo FP82H hot stage.

Single crystal data were collected on a Siemens SMART diffractometer, using the omega scan mode (Mo Kα λ = 0.71073 Å). Crystals were grown by cooling a saturated solution of **NDA-n_0** in 1,2-dichlorobenzene. Direct methods revealed all of the non-hydrogen atoms for **NDA-n_0** and all non-hydrogen atoms were refined anisotropically. The final least-squares refinement for **NDA-n_0** converged at the *R*-factor reported in Table 1. All calculations were performed using NRCVAX software.[22]

In order to study the redox behavior, dilute solutions of the ether-imide model compounds in tetrahydrofuran (freshly distilled from CaH_2) were examined using cyclic voltammetry. The measurements were conducted using a Platinum (PTE) working electrode in tetrahydrofuran containing 0.1 M tetrabutylammoniumhexafluorophosphate (TBAPF6). Nitrogen was bubbled through the solution to remove all traces of oxygen. The setup consisted of a three-electrode cell (BAS C-3 cell stand) and potentiostat assembly (BAS 100 B/W). The potentials were measured vs. Ag/AgCl as reference electrode and each measurement was calibrated with ferrocene as an internal standard.[21]

4.2. Materials. All common start materials and reagents were obtained from Aldrich Chemical Co. 3-Phenoxy-phenol was purchased from Alfa Aesar, pyromellitic dianhydride (**PMDA**), 3,3',4,4'-biphenyltetracarboxylic dianhydride (**BPDA**) from Chriskev Company Inc., and 3,3',4,4'-oxydiphthalic dianhydride (**OPDA**) was purchased from Occidental Chemical Corporation. Toluene and pyridine were dried over and distilled from CaH_2 prior to use.

From the aryl-ether amines used in this study, only 4-phenoxy-phenylamine was commercially available. 4-(3-Phenoxy-phenoxy)-phenylamine (**2**) and 4-(3-phenoxy-3-phenoxy-phenoxy)-phenylamine (**4**), however, were synthesized using standard ether synthesis procedures as show in Scheme 1.

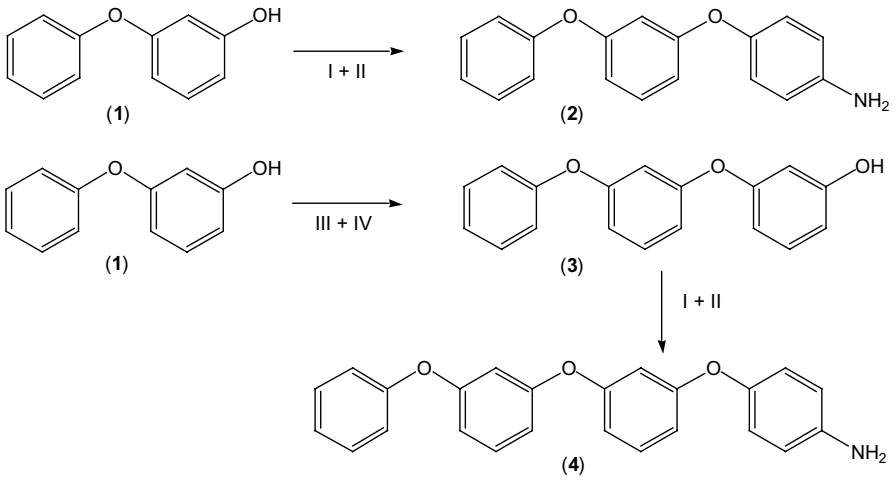

I: DMAc/K_2CO_3 and 1-fluoro-4-nitrobenzene, reflux for 12 h.
II: THF and 10% Pd-C/H_2, room temperature for 4 h.
III: Toluene/NaOMe and 3-bromoanisole/pyridine/CuCl, reflux for 12 h.
IV: HOAc and 48% HBr, reflux for 12 h.

SCHEME 1. *Synthesis of 4-(3-phenoxy-phenoxy)-phenylamine (**2**) and 4-(3-phenoxy-3-phenoxy-phenoxy)-phenylamine (**4**).*

4-(3-Phenoxy-phenoxy)-phenylamine (**2**) was conveniently prepared in two steps by the aromatic nucleophilic displacement reaction of 3-phenoxy-phenol with 1-fluoro-4-nitrobenzene [23]. The obtained 1-(4-nitro-phenoxy)-3-phenoxy-benzene was reduced to the corresponding amine using 10% Pd/C in a hydrogen atmosphere at room temperature. The synthesis of 4-(3-Phenoxy-3-phenoxy-phenoxy)-phenylamine (**4**) proved to be more elaborate. In the first step the intermediate 3-(3-phenoxy-phenoxy)-anisole was synthesized in good yields using standard Ullmann condensation techniques.[24-26] After cleaving the methoxy group with HBr [26], the 3-(3-phenoxy-phenoxy)-phenol (**3**) was treated with 1-

fluoro-4-nitrobenzene in the presence of potassium carbonate, and after reducing the nitro group the desired amine (**4**) was obtained.

4.3. Synthesis.

4.3.1. 4-(3-Phenoxy-phenoxy)-phenylamine (2) A 300 ml 2-neck flask equipped with an overhead stirrer, nitrogen inlet, and a Dean-Stark trap with condenser was charged with 9.31 g (0.05 mol) 3-phenoxy-phenol (**1**), 7.6 g (0.055 mol) finely ground K_2CO_3, 100 ml DMAc, and 100 ml toluene. This mixture was stirred and heated at 135 ^oC for 1.5 h., after which the temperature was increased to 175 ^oC. The theoretical amount of water was collected in the Dean-Stark trap and removed together with the toluene. The dark reaction mixture was cooled to room temperature, 9.2 g (0.065 mol) 1-fluoro-4-nitrobenzene was added, and this mixture was heated to 160 ^oC overnight. After the reaction mixture was cooled to room temperature, 100 ml of a 15% HCl solution was slowly added. This mixture was extracted with CH_2Cl_2 (3X) and the organic layer was washed with water (2X) and dried over $MgSO_4$. After removing the solvent a dark yellow oil was obtained, which was purified using a Kugel-Rohr apparatus. 1-(4-Nitro-phenoxy)-3-phenoxy-benzene was obtained as a bright yellow oil at 180 ^oC/55 mTorr, and this material was recrystallized once from acetone (-20 ^oC). Yield: 10.0 g (65%); mp 54 ^oC; TLC (9/1 hexane/ethyl acetate) t_r=0.5.

A 150 ml hydrogenation bottle was charged with 6.5 g (0.021 mol) 1-(4-nitro-phenoxy)-3-phenoxy-benzene, 75 ml dry THF, and 0.35 g 10% Pd-C. The bottle was placed in a Parr-hydrogenator and the nitro group was reduced under H_2-atmosphere (50 psi) at room temperature. The THF solution was filtered over a short silica-gel/celite patch and the THF was removed by distillation. A yellow oil was obtained and used without further work-up. Yield: 5.7 g (97%); TLC (9/1 hexane/ethyl acetate) t_r=0.1 (one spot); ^{1}H-NMR ($CDCl_3$) δ (ppm): 3.85 (s, 2H), 6.65 (d, 2H, *J*=8.8Hz), 6.61-6.68 (m, 3H), 6.88 (d, 2H, *J*=8.8Hz), 7.02 (dd, 2H, *J*=8.7Hz), 7.09 (t, 1H, *J*=7.4Hz), 7.19 (t, 1H, *J*=9Hz), 7.32 (tt, 2H, *J*=7.5Hz); ^{13}C-NMR ($CDCl_3$) δ (ppm): 107.84, 111.59, 112.02, 116.12, 119.0, 119.44, 121.22, 123.37, 129.67, 130.09, 142.93, 147.91, 156.72, 158.39, 160.27.

4.3.2. 4-(3-Phenoxy-3-phenoxy-phenoxy)-phenylamine (4) A 200 ml 2-neck flask equipped with a stir bar, a nitrogen inlet, and distillation apparatus, was charged with 4.73 g (0.0875 mol) sodium methoxide and 100 ml dry toluene. Using an addition funnel, 16.76 g (0.09 mol) 3-phenoxy-phenol (**1**) was slowly added and after the reaction was completed, the reaction mixture was heated and the methanol and toluene were distilled off leaving a white phenoxy salt. The salt was cooled to room temperature, a reflux condenser was fitted on the flask and, 100 ml dry pyridine were added. This solution was heated to reflux and in a stream of nitrogen, 25.25 g (0.135 mol) 3-bromoanisole was added all at once, followed immediately by 1.35 g (0.014 mol) CuCl. This reaction mixture was stirred at reflux for 12 h. and cooled to room temperature. The reaction was quenched with 80 ml, 15% HCl and extracted with diethyl ether (3X). The organic layer was washed with water and dried over $MgSO_4$. The dry ether solution was filtered over a short patch of silica-gel/celite to remove the copper salts. The solvent and excess 3-phenoxy-phenol and 3-bromoaniline were removed by vacuum distillation, and the remaining red oil was chromatographed over a short silica-gel column using hexane/ethyl acetate (9/1). After removing the solvent, 3-(3-phenoxy-phenoxy)-anisole was collected as a pale yellow oil. Yield: 15.3 g (58%); TLC (9/1 hexane/ethyl acetate) t_r=0.46 (one spot); MS (*m/z*): 292 (M+), 249, 171, 141, 128, 115.

A 200 ml one-neck flask equipped with stir bar and reflux condenser was charged with 15 g (0.05 mol) 3-(3-phenoxy-phenoxy)-anisole, 150 ml glacial acetic acid, and 80 ml HBr (48%). This solution was refluxed for 14 h. and allowed to cool to room temperature. The orange solution was extracted with CH_2Cl_2 and the organic layer was washed with water (2X) and dried over $MgSO_4$. The solvent was removed and the 3-(3-phenoxy-phenoxy)-phenol (**3**) was used for the next step without further purification. Yield: 13.5 g (94%); TLC (9/1 hexane/ethyl acetate) t_r=0.17 (one spot).

A 300 ml 2-neck flask equipped with an overhead stirrer, nitrogen inlet, and a Dean-Stark trap with condenser was charged with 14.3 g (0.05 mol) 3-(3-phenoxy-phenoxy)-phenol (**3**), 7.6 g (0.055 mol) finely ground K_2CO_3, 100 ml DMAc, and 100 ml toluene. This mixture was stirred and heated at 135 ^oC for 1.5 h., after which the temperature was increased to 175 ^oC. The theoretical amount of water was

collected in the Dean-Stark trap and removed together with the toluene. The dark reaction mixture was cooled to room temperature and 9.2 g (0.065 mol) 1-fluoro-4-nitrobenzene was added. This mixture was heated to 160 ^{o}C overnight. After the reaction mixture was cooled to room temperature, 100 ml of a 15% HCl solution was slowly added. This mixture was extracted with CH_2Cl_2 (3X) and the organic layer was washed with water (2X), and dried over $MgSO_4$. After removing the solvent, a dark yellow oil was obtained, which was dissolved in toluene. The toluene solution was chromatographed over a short silica-gel column with toluene as eluent, and after removing the toluene a bright yellow crystalline mass was obtained. 1-(4-nitro-3-phenoxy-phenoxy)-3-phenoxy-benzene was obtained as pale yellow crystals from acetone (-20 ^{o}C). Yield: 11.2 g (70%); mp 85-87 ^{o}C; TLC (9/1 hexane/ethyl acetate) t_r=0.27.

A 150 ml hydrogenation bottle was charged with 11 g (0.028 mol) 1-(4-nitro-3-phenoxy-phenoxy)-3-phenoxy-benzene, 100 ml dry THF, and 0.6 g 10% Pd-C. The bottle was placed in a Parr-hydrogenator and the nitro group was reduced under H_2-atmosphere (60 psi) at room temperature. The THF solution was filtered over a short silica-gel/celite patch and the THF was removed by distillation. A yellow oil was obtained and used without further work-up. Yield: 9.85 g (95%); TLC (9/1 hexane/ethyl acetate) t_r=0.04 (one spot); ^{1}H-NMR ($CDCl_3$) δ (ppm): 6.65-6.76 (m, 7H), 6.78 (t, 1H, *J*=2.1Hz), 6.91 (d, 2H, *J*=4.4Hz), 7.08 (d, 2H, *J*=8.8Hz), 7.15 (t, 1H, *J*=7.4Hz), 7.24 (t, 1H, *J*=7.9Hz), 7.28 (t, 1H, *J*=8.1Hz), 7.38 (t, 2H, *J*=7.6Hz); ^{13}C-NMR ($CDCl_3$) δ (ppm): 108.33, 109.63, 112.24, 112.57, 113.52, 113.55, 116.39, 119.37, 121.49, 123.79, 129.98, 130.40, 130.55, 143.19, 148.15, 156.83, 158.06, 158.41, 158.81, 160.54.

4.4. Synthesis of the ether-imide model compounds.

All low-molecular weight ether-imide model compounds were synthesized as outlined in Scheme 2. The amic acid intermediate was formed in the initial room temperature step, and when the temperature was raised to reflux, the amic acid was dehydrated to the corresponding imide. Although the reaction appeared to be finished after 4 hours, as determined by TLC, we refluxed the reaction mixture overnight for convenience. The desired products often crystallized from the reaction mixture upon cooling.

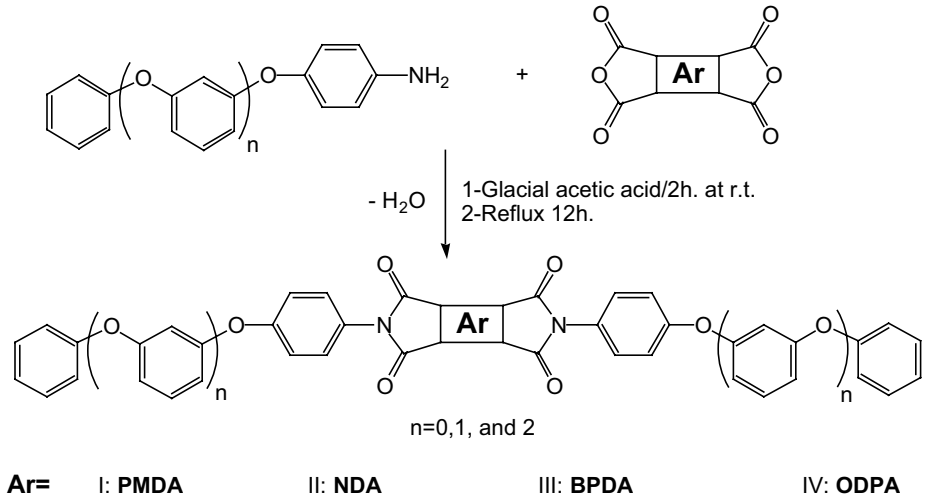

SCHEME 2. *Synthesis of the ether-imide model compounds*

4.4.1. Representative procedure for the synthesis of PMDA-n$_0$ A 50 ml one-neck flask equipped with a magnetic stir bar and reflux condenser was charged with pyromellitic dianhydride (0.57 g, 2.6 mmol), 4-phenoxy-phenylamine (1 g, 5.4 mmol), and 20 ml glacial acetic acid. This mixture was stirred for 2 h. at room temperature followed by heating at reflux (12 h.). Upon cooling bright yellow crystals formed, which were collected by filtration. The crude product was dissolved in a minimum amount of hot 1,2-dichlorobenzene and chromatographed over a short, heated, silica-gel patch. Pure

PMDA-n_0 was obtained after crystallization from hot 1,2-dichlorobenzene. Yield: 1.24 g (86%); ^{1}H-NMR (DMSO-d_6 at 125 ^{o}C) δ (ppm): 7.10-7.22 (m, 10H), 7.41 (t, 4H, *J*=6Hz), 7.53 (d, *J*=9Hz, 4H), 8.32 (s, 2H); FT-IR (KBr): 1723 (C=O_{imide}), 1785 (C=O_{imide}) cm^{-1}

4.4.2. Analytical data of NDA-n_0 Yield: 0.65 g (83%) recrystallized from CH_2Cl_2; t_r = 0.1 (CH_2Cl_2) one spot; ^{1}H-NMR (DMSO-d_6 at 125 ^{o}C) δ (ppm): 7.13-7.23 (m, 10H), 7.42-7.48 (m, 8H), 8.75 (s, 4H); ^{13}C-NMR (DMSO-d_6 at 125 ^{o}C) δ (ppm): 117.75, 118.34, 122.99, 126.17, 126.36, 129.14, 129.69, 129.72, 155.89, 156.36, 161.97; FT-IR (KBr): 1712 (C=O_{imide}) cm^{-1}

4.4.3. Analytical data of BPDA-n_0 Yield: 1.52 g (93%) recrystallized from CH_2Cl_2; t_r = 0.11 (CH_2Cl_2) one spot; ^{1}H-NMR ($CDCl_3$) δ (ppm): 7.06-7.17 (m, 10H), 7.34-7.41 (m, 8H), 8.09 (dd, 4H), 8.22 (s, 2H); ^{13}C-NMR ($CDCl_3$) δ (ppm): 119.07, 119.81, 122.80. 124.20, 124.88, 126.33, 128.21, 130.14, 131.81, 133.20, 133.58, 145.65, 156.63, 157.62, 167.02, 167.06; FT-IR (KBr): 1711 (C=O_{imide}), 1774 (C=O_{imide}) cm^{-1}

4.4.4. Analytical data of ODPA-n_0 Yield: 1.31 g (78%) recrystallized from 1,2-dichloro benzene; t_r = 0.16 (CH_2Cl_2) one spot; ^{1}H-NMR ($CDCl_3$) δ (ppm): 7.09-7.21 (m, 10H), 7.40-7.48 (m, 8H), 7.62 (dd, 4H, *J*=11.8Hz), 8.03 (dd, 2H, *J*=8.7Hz); FT-IR (KBr): 1709 (C=O_{imide}), 1777 (C=O_{imide}) cm^{-1}

4.4.5. Analytical data of PMDA-n_1 Yield: 1.25 g (88%) recrystallized from 1,2-dichloro benzene; t_r = 0.25 (CH_2Cl_2) one spot; ^{1}H-NMR (DMSO-d_6 at 125 ^{o}C) δ (ppm): 6.73 (t, 2H, *J*=2.3 Hz), 6.83 (tt, 4H, *J*=8.3 Hz), 7.06 (d, 4H, *J*=8.8 Hz), 7.15-7.22 (m, 6H), 7.37-7.43 (m, 6H), 7.53 (d, 4H, *J*=8.9 Hz), 8.32 (s, 2H); ^{13}C-NMR (DMSO-d_6 at 125 ^{o}C) δ (ppm): 108.70, 112.92, 113.06, 117.10, 118.11, 118.17, 122.93, 126.43, 127.75, 129.05, 130.09, 136.38, 155.72, 157.07, 157.82, 164.33; FT-IR (KBr): 1723 (C=O_{imide}), 1785 (C=O_{imide}) cm^{-1}

4.4.6. Analytical data of NDA-n_1 Yield: 1.12 g (85%) recrystallized from CH_2Cl_2; t_r = 0.13 (CH_2Cl_2) one spot; ^{1}H-NMR ($CDCl_3$) δ (ppm): 6.79-6.87 (m, 6H), 7.06 (d, 4H, *J*=8.7 Hz), 7.14-7.20 (m, 6H), 7.28-7.40 (m, 11H), 8.85 (s, 4H); ^{13}C-NMR ($CDCl_3$) δ (ppm): 110.52, 114.27, 114.33, 119.31, 119.54, 124.0, 127.22, 127.39, 129.33, 130.09, 130.52, 131.71, 156.75, 157.68, 157.93, 159.16, 163.25; FT-IR (KBr): 1717 (C=O_{imide}) cm^{-1}

4.4.7. Analytical data of BPDA-n_1 Yield: 1.24 g (90%) recrystallized from CH_2Cl_2; t_r = 0.20 (CH_2Cl_2) one spot; ^{1}H-NMR ($CDCl_3$) δ (ppm): 6.75-6.81 (m, 3H), 7.05 (dd, 4H, *J*=7.6 Hz), 7.12-7.17 (m, 6H), 7.17-750 (m, 10H), 8.10 (dd, 4H, *J*=2 Hz), 8.24 (s, 2H); ^{13}C-NMR ($CDCl_3$) δ (ppm): 110.33, 114.16, 114.24, 119.52, 119.71, 123.0, 124.17, 125.08, 126.85, 128.39, 130.26, 130.95, 131.97, 133.35, 133.79, 145.83, 156.92, 157.22, 158.14, 159.29, 167.14, 167.19; FT-IR (KBr): 1719 (C=O_{imide}), 1774 (C=O_{imide}) cm^{-1}

4.4.8. Analytical data of ODPA-n_1 Yield: 1.41 g (87%) recrystallized from CH_2Cl_2; t_r = 0.29 (CH_2Cl_2) one spot; ^{1}H-NMR ($CDCl_3$) δ (ppm): 6.70-6.81 (m, 6H), 7.05 (dd, 4H, *J*=8.7 Hz), 7.10-7.24 (m, 6H), 7.24-7.42 (m, 10H), 7.48 (dd, 2H, *J*=8.2 Hz), 7.55 (d, 2H, *J*=2 Hz), 8.0 (d, 2H, *J*=8 Hz); ^{13}C-NMR ($CDCl_3$) δ (ppm): 109.93, 113.76, 113.83, 113.98, 119.07, 119.29, 123.76, 124.83, 126.25, 126.41, 127.27, 127.99, 129.84, 130.53, 134.60, 156.50, 156.80, 157.70, 158.87, 161.18, 166.23, 166.37; FT-IR (KBr): 1711 (C=O_{imide}), 1774 (C=O_{imide}) cm^{-1}

4.4.9. Analytical data of PMDA-n_2 Yield: 1.12 g (93%) recrystallized from CH_2Cl_2; t_r = 0.31 (CH_2Cl_2) one spot; ^{1}H-NMR (DMSO-d_6 at 125 ^{o}C) δ (ppm): 6.65-6.88 (m, 12H), 7.03 (d, 4H, *J*=7.7Hz), 7.13-7.20 (m, 6H), 7.34-7.41 (m, 8H), 7.53 (d, 4H, *J*=8.9Hz), 8.31 (s, 2H); ^{13}C-NMR (DMSO-d_6 at 125 ^{o}C) δ (ppm): 108.42, 108.98, 112.76, 112.92, 113.35, 117.12, 118.14, 118.19, 122.93, 126.49, 127.79, 129.05, 130.02, 130.19, 133.62, 136.41, 155.69, 155.69, 157.12, 157.27, 157.78, 164.35; FT-IR (KBr): 1724 (C=O_{imide}), 1781 (C=O_{imide}) cm^{-1}

4.4.10. Analytical data of NDA-n_2 Yield: 1.11 g (88%) recrystallized from DMSO/EtOH; t_r = 0.1 (CH_2Cl_2) one spot; ^{1}H-NMR ($CDCl_3$) δ (ppm): 6.74-6.87 (m, 12H), 7.06 (d, 4H, *J*=9Hz), 7.13-7.22 (m, 6H), 7.28-7.39 (m, 12H), 8.87 (s, 4H); ^{13}C-NMR ($CDCl_3$) δ (ppm): 109.82, 110.78, 113.71, 113.83, 114.58, 114.70, 119.37, 119.50, 123.89, 127.22, 127.39, 129.40, 130.04, 130.09, 130.71, 130.87, 131.72, 156.81, 157.73, 157.84, 158.18, 158.53, 159.0, 163.24; FT-IR (KBr): 1717 (C=O_{imide}) cm^{-1}

4.4.11. Analytical data of BPDA-n$_2$ Yield: 1.17 g (90%) recrystallized from CH_2Cl_2; t_r = 0.25 (CH_2Cl_2) one spot; ^{1}H-NMR ($CDCl_3$) δ (ppm): 6.70-6.81 (m, 12H), 7.01-7.15 (m, 10H), 7.28-7.44 (m, 12H), 8.08 (dd, 4H, *J*=8.3Hz), 8.22 (s, 2H); ^{13}C-NMR ($CDCl_3$) δ (ppm): 109.77, 110.37, 113.67, 113.81, 114.32, 119.36, 119.45, 122.78, 123.87, 124.86, 126.74, 128.21, 130.02, 130.69, 130.82, 131.75, 133.13, 133.58, 145.59, 156.77, 156.90, 157.99, 158.13, 158,46, 158.94, 166.92, 166.96; FT-IR (KBr): 1721 ($C=O_{imide}$), 1774 ($C=O_{imide}$) cm^{-1}

4.4.12. Analytical data of ODPA-n$_2$ Yield: 1.26 g (96%) recrystallized from CH_2Cl_2; t_r = 0.3 (CH_2Cl_2) one spot; ^{1}H-NMR ($CDCl_3$) δ (ppm): 6.70-6.81 (m, 12H), 7.02-7.14 (m, 10H), 7.25-7.41 (m, 12H), 7.47 (dd, 2H, *J*=8.2Hz), 7.55 (d, 2H, *J*=2.1Hz), 8.01 (d, 2H, *J*=8.2Hz); ^{13}C-NMR ($CDCl_3$) δ (ppm) 109.78, 110.40, 113.68, 113.82, 114.19, 114.34, 119.34, 119.46, 123.88, 125.05, 126.46, 126.72, 127.49, 128.22, 130.03, 130.69, 130.83, 134.81, 156.77, 156.92, 157.98, 158.14, 158.46, 158.96, 161.39, 166.43, 166.56; FT-IR (KBr): 1709 ($C=O_{imide}$), 1777 ($C=O_{imide}$) cm^{-1}

Acknowledgements. This work was supported in part by the NASA University Research, Engineering and Technology Institute on Bio Inspired Materials (BIMat) under award No. NCC-1-02037. We thank Crystal Topping for performing the DSC measurements. Dr. Peter S. White and Dr. Jirakorn Thisayukta at the University of North Carolina at Chapel Hill are gratefully acknowledged for the X-ray diffraction studies.

REFERENCES

[1] R. J. COTTER, *Engineering plastics, A handbook of polyarylethers,* Gordon and Breach Publishers, 1995.
[2] M.K. GHOSH AND K.L. MITTAL, *Polyimides, fundamentals and applications,* Marcel Dekker, 1996.
[3] S.M. MACKINNON AND Z.Y. WANG, *J. Pol.Sci. Part A: Polym. Chem.*, 38 (2000), pp. 3467.
[4] F. WÜRTHNER, *Angew. Chem. Int. Ed.*, 40 (2001), pp. 1037.
[5] H.E. KATZ, A.J. LOVINGER, J. JOHNSON, C. KLOC, T. SIEGRIST, W. LI, Y.-Y. LIN, AND A. DODABALAPUR, *Nature,* 404 (2000), pp. 478.
[6] E. BIALECKA-FLORJANCZYK AND A. ORZESZKO, *J. Mater. Chem.*, 10 (2000), pp. 1527.
[7] P. EISELT, S. DENZINGER AND H. SCHMIDT, *Liq. Cryst.,* 18 (1995), pp. 257.
[8] K. JOW AND T. DINGEMANS, *Liq. Cryst.,* 29 (2002), pp. 573.
[9] P.J. COLLINGS AND M. HIRD, *Introduction to liquid crystals,* Taylor and Francis, 1997.
[10] C.J. BORRILL AND R.H. WHITELEY, *J. Mater. Chem.,* 2 (1992), pp. 997.
[11] P.J. HORNER AND R.H. WHITELEY, *J. Mater. Chem.,* 1 (1991), pp. 271.
[12] S.T. WELLINGHOFF, H. ISHIDA, J.L. KOENIG AND E. BAER, *Macromolecules,* 13 (1980), pp. 834.
[13] H. ISHIDA, S.T. WELLINGHOFF, E. BAER AND J.L. KOENIG, *Macromolecules,* 13 (1980), pp. 826.
[14] S.A. KAFAFI, J.P. LAFEMINA AND J.L. NAUSS, *J. Am. Chem. Soc.,* 112 (1990), pp. 8742.
[15] J.R. HAVENS, H. ISHIDA AND J.L. KOENIG, *Macromolecules,* 14 (1981), pp. 1327.
[16] J.M. ADDUCI, *Polym.Prepr.,* 31 (1990), pp. 63.
[17] T. DINGEMANS, N.S. MURTHY AND E.T. SAMULSKI, *J. Phys. Chem. B.,* 105 (2001), pp. 8845.
[18] H. ZHENG, C. K. LAI AND T. M. SWAGER, *Chem. Mater.,* 7 (1995), pp. 2067.
[19] R.M. SILVERSTEIN, G.C. BASSLER, AND T. C. MORRILL, *Spectrometric identification of organic compounds*, John Wiley & Sons, 1991.
[20] L. L. MILLER, B. ZINGER, AND J.S. SCHLECHTE, *Chem. Mater.*, 11 (1999), pp. 2313.
[21] J. POMMEREHNE, H. VESTWEBER, W. GUSS, R.F. MAHRT, H. BÄSSLER, M. PORSCH, AND J. DAUB, *Adv. Mater.*, 7 (1995), pp. 551.

[22] E.J. GABE, Y. LE PAGE, J.-P. CHARLAND, F.L. LEE AND P.S. WHITE, *J. Appl. Crystallogr.,* 22 (1989), pp. 384.
[23]G.C. EASTMOND AND J. PAPROTNY, *Synthesis,* (1998), pp. 894.
[24] A.A. MOROZ AND M.S. SHVARTSBERG, *Rus. Chem. Rev,* 43 (1974), pp. 679.
[25] A.L. WILLIAMS, R.E. KINNEY AND R.F. BRIDGER, *J.Org.Chem.*, 32 (1967), pp. 2501.
[26] K.J. SAX, W.S. SAARI, C.L. MAHONEY AND J.M. GORDON, *J.Org.Chem.*, 25 (1960), pp. 1590.

APPENDIX 1.

Phase behavior, transition temperatures (^{o}C) and enthalphy's (KJ mol^{-1}) (italic) for the aryl-ether terminated di-imide model compounds upon heating and cooling (10 ^{o}C.min^{-1}).

Name	T_g	K	K'	K''	D_r	S_A	I
PMDA n=0		• 327.6 (*8.9*) • 361.8 (*-2.0*)	• 387.4 (*60.8*) • 371.6 (*-60.5*)				• •
PMDA n=1		• 290.3 (*87.4*) • 286.7 (*-83.9*)					• •
PMDA n=2		• 233.3 (*81.8*) • 225.5 (*-78.2*)					• •
NDA n=0		• 344.7 (*52.9*) • 310.3 (*-23.5*)			• 333.3 (*-24.7*)	• 335.0 (*-8.0*)	• •
NDA n=1		• 267.3 (*70.1*) • 240.2 (*-45.6*)					• •
NDA n=2		• 232.4 (*84.8*) • 172.0 (*-60.5*)					• •
BPDA n=0		• 203.6 (*-5.6*) •	• 276.7 (*68.5*) 190.3 (*-46.3*)				• •
BPDA n=1	• 69.4 • 63.7	• 98.2 (*-27.2*)	• 134.7 (*-6.8*)	• 175.3 (*62.0*)			• •
BPDA n=2	• 60.8	• 145.3 (*69.3*)					• •
OPDA n=0		• 292.4 (*73.6*) • 244.0 (*-68.3*)					• •
ODPA n=1	• 150.6	• 161.9 (*-7.7*) • 141.4 (*-41.9*)	• 185.2 (*46.3*)				• •
OPPA n=2	• 60.3 • 56.4	• 115.4 (*-35.9*)	• 143.3 (*37.2*)				• •

Tg= glass transition temperature, K= crystal phase, D_{rd}= rectangular columnar phase, S_A= smectic A phase, and I= isotropic phase

APPENDIX 2.
Crystal data and structure refinement for ***NDA-n$_0$***.

	NDA-n$_0$
empirical formula	$C_{38}H_{22}N_2O_6$
formula weight (g mol^{-1})	602.60
temperature (K)	298
crystal system	monoclinic
color of crystal	yellow
space group	$P\ 2_1/n$
unit cell dimensions	
a (Å)	7.5736(15)
b (Å)	5.2290(10)
c (Å)	35.678(7)
β (deg)	91.251(1)
volume (Å^3)	1412.6(5)
Z	2
F(000)	624.40
crystal size (mm)	0.40 x 0.30 x 0.05
θ range for data collection (deg)	5 to 50
limiting indices	
	$-9 \leq h \leq 9$
	$0 \leq k \leq 6$
	$0 \leq l \leq 42$
reflections collected	12985
independent reflections	2493
refinement method	full matrix least-squares on F^2
data/restraints/parameters	
goodness of fit on F^2	1.9410
R1	0.068
wR2	0.073
R indices (all data)	
R1	0.108
wR2	0.122

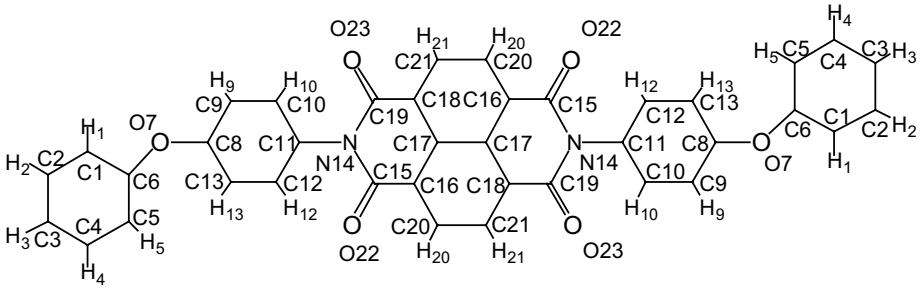

Atomic Parameters x,y,z and Biso.
E.S.Ds. refer to the last digit printed.

	x	y	z	Biso
C1	0.5837(5)	0.7544(9)	0.17961(11)	1.93(18)
C2	0.7180(6)	0.5820(8)	0.18725(12)	2.15(19)
C3	0.6981(6)	0.3923(8)	0.21354(12)	2.06(18)
C4	0.5397(6)	0.3753(9)	0.23270(12)	2.35(19)
C5	0.4053(6)	0.5455(8)	0.22526(11)	1.97(19)
C6	0.4287(5)	0.7323(8)	0.19893(10)	1.58(16)
O7	0.2941(3)	0.9136(5)	0.19358(7)	2.08(11)
C8	0.1862(5)	0.8987(7)	0.16198(10)	1.32(15)
C9	0.1952(5)	0.7065(8)	0.13539(11)	1.64(17)
C10	0.0777(5)	0.7096(8)	0.10477(10)	1.62(16)
C11	-0.0438(5)	0.9035(8)	0.10149(10)	1.48(16)
C12	-0.0545(5)	1.0944(8)	0.12812(11)	1.65(17)
C13	0.0632(5)	1.0905(8)	0.15835(11)	1.69(17)
N14	-0.1678(4)	0.9120(6)	0.06968(8)	1.46(13)
C15	-0.3118(5)	0.7412(8)	0.06934(10)	1.43(16)
C16	-0.4516(5)	0.7834(7)	0.04046(9)	1.19(16)
C17	-0.4317(5)	0.9801(7)	0.01370(9)	1.13(15)
C18	-0.2801(5)	1.1361(7)	0.01328(10)	1.26(16)
C19	-0.1387(5)	1.0975(7)	0.04224(10)	1.41(16)
C20	-0.5992(5)	0.6325(8)	0.04009(10)	1.54(17)
C21	-0.2644(5)	1.3254(8)	-0.01304(10)	1.51(16)
O22	-0.3192(4)	0.5700(5)	0.09236(8)	2.26(12)
O23	-0.0025(3)	1.2229(5)	0.04286(7)	2.02(12)
H1	0.599 (5)	0.896 (8)	0.1624 (11)	2.6 (9)
H2	0.835 (6)	0.607 (8)	0.1728 (12)	3.9 (11)
H3	0.794 (5)	0.261 (8)	0.2205 (11)	3.0 (10)
H4	0.525 (5)	0.233 (9)	0.2520 (11)	2.9 (10)
H5	0.296 (5)	0.547 (7)	0.2370 (10)	1.5 (8)
H9	0.281 (5)	0.585 (7)	0.1385 (10)	1.4 (8)
H10	0.079 (5)	0.555 (8)	0.0863 (12)	3.1 (10)
H12	-0.145 (5)	1.235 (8)	0.1243 (10)	2.4 (9)
H13	0.066 (5)	1.217 (7)	0.1752 (10)	1.2 (8)
H20	-0.610 (5)	0.487 (8)	0.0593 (11)	3.1 (10)
H21	-0.163 (5)	1.437 (7)	-0.0128 (10)	1.7 (8)

Biso is the Mean of the Principal Axes of the Thermal Ellipsoid

u(i,j) or U values *100.
E.S.Ds. refer to the last digit printed

	u11(U)	u22	u33	u12	u13	u23
C1	2.8 (3)	2.6 (3)	1.92(21)	0.06(20)	0.06(19)	-0.04(19)
C2	1.95(24)	3.4 (3)	2.82(23)	0.18(21)	-0.07(19)	-0.28(21)
C3	2.2 (3)	2.51(25)	3.05(24)	0.38(21)	-0.81(20)	-0.42(20)
C4	3.2 (3)	3.0 (3)	2.73(24)	-0.24(22)	-0.34(20)	0.76(21)
C5	1.40(24)	3.4 (3)	2.68(24)	-0.09(20)	0.12(20)	0.19(20)
C6	1.97(23)	2.35(23)	1.67(20)	0.41(18)	-0.63(17)	-0.33(18)
O7	2.30(17)	3.37(17)	2.18(15)	1.00(14)	-0.92(12)	-0.71(13)
C8	1.42(22)	1.67(21)	1.92(21)	-0.28(17)	-0.27(17)	0.32(18)
C9	1.38(22)	2.42(24)	2.42(23)	0.53(19)	-0.21(18)	0.26(20)
C10	1.94(23)	2.26(23)	1.95(21)	0.08(19)	0.19(18)	-0.20(19)
C11	1.50(22)	2.51(23)	1.59(20)	-0.56(18)	-0.37(17)	0.47(18)
C12	1.89(24)	2.08(22)	2.29(22)	0.14(19)	0.01(18)	0.42(20)
C13	2.41(25)	2.12(23)	1.87(21)	-0.22(20)	-0.23(18)	-0.39(20)
N14	1.72(19)	2.18(18)	1.62(17)	-0.32(15)	-0.42(14)	0.61(15)
C15	1.78(23)	2.11(23)	1.53(19)	0.01(18)	0.32(17)	0.01(19)
C16	1.30(21)	2.03(21)	1.19(19)	-0.10(18)	-0.01(16)	0.03(17)
C17	1.31(21)	1.84(21)	1.16(18)	0.13(17)	0.10(15)	0.01(17)
C18	1.49(22)	2.05(22)	1.25(19)	-0.02(17)	-0.02(16)	0.07(17)
C19	2.03(24)	2.00(22)	1.33(20)	-0.10(19)	-0.10(17)	-0.03(18)
C20	1.85(23)	2.47(24)	1.52(20)	-0.07(19)	-0.02(18)	0.25(18)
C21	1.77(23)	2.12(23)	1.86(21)	-0.43(19)	0.17(18)	0.29(18)
O22	2.49(17)	3.08(17)	3.00(16)	-0.45(14)	-0.62(13)	1.38(15)
O23	1.69(16)	19(17)	2.77(16)	-0.92(14)	-0.69(12)	0.69(14)
H1	3.3(12)					
H2	5.0(14)					
H3	3.9(12)					
H4	3.7(12)					
H5	2.0(10)					
H9	1.8(10)					
H10	4.0(12)					
H12	3.0(11)					
H13	1.6(10)					
H20	3.9(13)					
H21	2.2(11)					

Anisotropic Temperature Factors are of the form
Temp=-2*Pi*Pi*(h*h*u11*astar*astar+---+2*h*k*u12*astar*bstar+---)

DISANG -- The NRCVAX Distance and Angle Program

The Space Group is P 21/N Centrosymmetric
The Equivalent Positions are:
1) x y z 2) 1/2-x 1/2+y 1/2-z

The Lattice is Primitive. There are no Centering Vectors

There are Symmetry Equivalent atoms.
The Bond and Angle Tables may need editing.

The following Atoms are the Symmetry Equivalents

Name	x	y	z			
C(17)a	-0.56827	1.01988	-0.01370	-1.000-x	2.000-y	-z
C(21)a	-0.73559	0.67462	0.01304	-1.000-x	2.000-y	-z
C(20)a	-0.40084	1.36753	-0.04009	-1.000-x	2.000-y	-z

C(1)-C(2)	1.381(6)	C(11)-N(14)	1.458(5)
C(1)-C(6)	1.379(6)	C(12)-C(13)	1.384(6)
C(1)-H(1)	0.97(4)	C(12)-H(12)	1.01(4)
C(2)-C(3)	1.376(6)	C(13)-H(13)	0.89(4)
C(2)-H(2)	1.04(5)	N(14)-C(15)	1.410(5)
C(3)-C(4)	1.397(6)	N(14)-C(19)	1.399(5)
C(3)-H(3)	1.02(4)	C(15)-C(16)	1.478(5)
C(4)-C(5)	1.374(6)	C(15)-O(22)	1.217(5)
C(4)-H(4)	1.02(4)	C(16)-C(17)	1.414(5)
C(5)-C(6)	1.370(6)	C(16)-C(20)	1.368(5)
C(5)-H(5)	0.94(4)	C(17)-C(17)a	1.423(7)
C(6)-O(7)	1.402(5)	C(17)-C(18)	1.409(5)
O(7)-C(8)	1.380(4)	C(18)-C(19)	1.486(5)
C(8)-C(9)	1.385(6)	C(18)-C(21)	1.371(5)
C(8)-C(13)	1.373(6)	C(19)-O(23)	1.222(5)
C(9)-C(10)	1.394(5)	C(20)-C(21)a	1.415(5)
C(9)-H(9)	0.92(4)	C(20)-H(20)	1.03(4)
C(10)-C(11)	1.372(6)	C(21)-C(20)a	1.415(5)
C(10)-H(10)	1.04(4)	C(21)-H(21)	0.97(4)
C(11)-C(12)	1.382(6)		

C(2)-C(1)-C(6) 118.5(4)
C(2)-C(1)-H(1) 121.7(24)
C(6)-C(1)-H(1) 119.7(24)
C(1)-C(2)-C(3) 120.9(4)
C(1)-C(2)-H(2) 116.7(24)
C(3)-C(2)-H(2) 122.4(24)
C(2)-C(3)-C(4) 119.2(4)
C(2)-C(3)-H(3) 124.1(23)
C(4)-C(3)-H(3) 116.8(23)
C(3)-C(4)-C(5) 120.3(4)
C(3)-C(4)-H(4) 118.9(22)
C(5)-C(4)-H(4) 120.8(22)
C(4)-C(5)-C(6) 119.2(4)
C(4)-C(5)-H(5) 125.4(22)
C(6)-C(5)-H(5) 115.4(22)
C(1)-C(6)-C(5) 121.8(4)
C(1)-C(6)-O(7) 120.0(4)
C(5)-C(6)-O(7) 118.1(4)
C(6)-O(7)-C(8) 119.3(3)
O(7)-C(8)-C(9) 124.3(3)
O(7)-C(8)-C(13) 115.1(3)
C(9)-C(8)-C(13) 120.6(3)
C(8)-C(9)-C(10) 119.3(4)
C(8)-C(9)-H(9) 117.8(22)
C(10)-C(9)-H(9) 123.0(22)
C(9)-C(10)-C(11) 119.4(4)
C(9)-C(10)-H(10) 118.2(22)
C(11)-C(10)-H(10) 122.2(22)
C(10)-C(11)-C(12) 121.6(3)
C(10)-C(11)-N(14) 120.5(3)
C(12)-C(11)-N(14) 117.8(3)
C(11)-C(12)-C(13) 118.6(4)
C(11)-C(12)-H(12) 118.7(22)
C(13)-C(12)-H(12) 122.7(22)
C(8)-C(13)-C(12) 120.6(4)
C(8)-C(13)-H(13) 118.0(22)
C(12)-C(13)-H(13) 121.3(22)
C(11)-N(14)-C(15) 118.2(3)
C(11)-N(14)-C(19) 117.2(3)
C(15)-N(14)-C(19) 124.5(3)
N(14)-C(15)-C(16) 117.0(3)
N(14)-C(15)-O(22) 120.5(3)
C(16)-C(15)-O(22) 122.5(3)
C(15)-C(16)-C(17) 119.6(3)
C(15)-C(16)-C(20) 119.6(3)
C(17)-C(16)-C(20) 120.8(3)
C(16)-C(17)-C(17)a 118.9(3)
C(16)-C(17)-C(18) 121.8(3)
C(17)a-C(17)-C(18) 119.2(3)
C(17)-C(18)-C(19) 119.3(3)
C(17)-C(18)-C(21) 120.5(3)
C(19)-C(18)-C(21) 120.2(3)
N(14)-C(19)-C(18) 117.3(3)
N(14)-C(19)-O(23) 120.4(3)
C(18)-C(19)-O(23) 122.3(3)
C(16)-C(20)-C(21)a 120.0(4)
C(16)-C(20)-H(20) 119.7(22)
C(21)a-C(20)-H(20) 120.3(22)
C(18)-C(21)-C(20)a 120.4(4)
C(18)-C(21)-H(21) 120.8(21)
C(20)a-C(21)-H(21) 118.7(21)

Torsion angles

C6	C1	C2	C3	0.0(4)	C6	C1	C2	H2	-178. (4)
H1	C1	C2	C3	176. (4)	H1	C1	C2	H2	-2. (6)
C2	C1	C6	C5	0.1(4)	C2	C1	C6	O7	176.0(9)
H1	C1	C6	C5	-176. (4)	H1	C1	C6	O7	0. (4)
C1	C2	C3	C4	-0.1(4)	C1	C2	C3	H3	-179. (4)
H2	C2	C3	C4	178. (4)	H2	C2	C3	H3	-1. (6)
C2	C3	C4	C5	0.2(4)	C2	C3	C4	H4	179. (4)
H3	C3	C4	C5	180. (4)	H3	C3	C4	H4	-1. (6)
C3	C4	C5	C6	-0.2(4)	C3	C4	C5	H5	-180. (4)
H4	C4	C5	C6	-179. (4)	H4	C4	C5	H5	1. (6)
C4	C5	C6	C1	0.0(4)	C4	C5	C6	O7	-175.9(9)
H5	C5	C6	C1	180. (4)	H5	C5	C6	O7	4. (4)
C1	C6	O7	C8	78.4(6)	C5	C6	O7	C8	-105.6(7)
C6	O7	C8	C9	3.4(4)	C6	O7	C8	C13	-177.3(8)
O7	C8	C9	C10	179.2(8)	O7	C8	C9	H9	-3. (4)
C13	C8	C9	C10	0.0(4)	C13	C8	C9	H9	178. (4)
O7	C8	C13	C12	-179.0(9)	O7	C8	C13	H13	5. (4)
C9	C8	C13	C12	0.3(4)	C9	C8	C13	H13	-176. (4)
C8	C9	C10	C11	0.3(4)	C8	C9	C10	H10	-175. (4)
H9	C9	C10	C11	-178. (4)	H9	C9	C10	H10	7. (6)
C9	C10	C11	C12	-1.0(4)	C9	C10	C11	N14	179.8(8)
H10	C10	C11	C12	174. (4)	H10	C10	C11	N14	-5. (4)
C10	C11	C12	C13	1.3(4)	C10	C11	C12	H12	179. (4)
N14	C11	C12	C13	-179.5(8)	N14	C11	C12	H12	-2. (4)
C10	C11	N14	C15	75.5(6)	C10	C11	N14	C19	-107.0(7)
C12	C11	N14	C15	-103.8(7)	C12	C11	N14	C19	73.7(6)
C11	C12	C13	C8	-0.9(4)	C11	C12	C13	H13	175. (4)
H12	C12	C13	C8	-179. (4)	H12	C12	C13	H13	-3. (6)
C11	N14	C15	C16	169.6(7)	C11	N14	C15	O22	-9.4(3)
C19	N14	C15	C16	-7.7(4)	C19	N14	C15	O22	173.2(8)
C11	N14	C19	C18	-170.0(7)	C11	N14	C19	O23	9.1(3)
C15	N14	C19	C18	7.4(4)	C15	N14	C19	O23	-173.5(8)
N14	C15	C16	C17	3.2(3)	N14	C15	C16	C20	-176.4(8)
O22	C15	C16	C17	-177.7(8)	O22	C15	C16	C20	2.6(4)
C15	C16	C17	C18	1.1(4)	C20	C16	C17	C18	-179.3(8)
C15	C16	C20	H20	-2. (4)	C17	C16	C20	H20	178. (4)
C16	C17	C18	C19	-1.4(4)	C16	C17	C18	C21	179.9(8)
C17	C18	C19	N14	-2.6(3)	C17	C18	C19	O23	178.4(8)
C21	C18	C19	N14	176.1(8)	C21	C18	C19	O23	-3.0(4)
C17	C18	C21	H21	177. (4)	C19	C18	C21	H21	-1. (4)

REPORT DOCUMENTATION PAGE

Form Approved
OMB No. 0704-0188

1. AGENCY USE ONLY *(Leave blank)*	2. REPORT DATE	3. REPORT TYPE AND DATES COVERED
	December 2002	Contractor Report

4. TITLE AND SUBTITLE
WHOLLY AROMATIC ETHER-IMIDES. POTENTIAL MATERIALS FOR *n*-TYPE SEMICONDUCTORS

5. FUNDING NUMBERS
C NAS1-97046
WU 505-90-52-01

6. AUTHOR(S)
Theo J. Dingemans, Terry L. St Clair, and Edward T. Samulski

7. PERFORMING ORGANIZATION NAME(S) AND ADDRESS(ES)
ICASE
Mail Stop 132C
NASA Langley Research Center
Hampton, VA 23681-2199

8. PERFORMING ORGANIZATION REPORT NUMBER
ICASE Report No. 2002-47

9. SPONSORING/MONITORING AGENCY NAME(S) AND ADDRESS(ES)
National Aeronautics and Space Administration
Langley Research Center
Hampton, VA 23681-2199

10. SPONSORING/MONITORING AGENCY REPORT NUMBER
NASA/CR-2002-212135
ICASE Report No. 2002-47

11. SUPPLEMENTARY NOTES
Langley Technical Monitor: Dennis M. Bushnell
Final Report
To be submitted to Chemistry of Materials.

12a. DISTRIBUTION/AVAILABILITY STATEMENT
Unclassified–Unlimited
Subject Category 34
Distribution: Nonstandard
Availability: NASA-CASI (301) 621-0390

12b. DISTRIBUTION CODE

13. ABSTRACT *(Maximum 200 words)*

We report on the synthesis and characterization of a novel series low-molar-mass ether-imide rod-shaped model compounds. All ether-imides were obtained by terminating the appropriate rigid core dianhydride, i.e. pyromellitic dianhydride (PMDA), 1,4,5,8-naphthalenetetracarboxylic dianhydride (NDA), 3,3',4,4'-biphenyltetracarboxylic dianhydride (BPDA), and 3,3',4,4'-oxydiphthalic dianhydride (ODPA) with three flexible aryl-ether tails of different chain length. The mono-functional aryl-ether amines, i.e. 4-(3-phenoxy-phenoxy)-phenylamine (2) and 4-(3-phenoxy-3-phenoxy-phenoxy)-phenylamine (4), were synthesized using standard fluoro-displacement and Ullmann condensation techniques. The corresponding ether-imide model compounds were obtained in high yields using a one-step solution imidization procedure. Increasing the number of meta-substituted aryl-ether units reduces the melt transition temperatures and at the same time it increases the solubility of the model compounds. Most model compounds are crystalline solids and form isotropic melts upon heating. 2,7-Bis-(-4-phenoxy-phenyl)-benzo[lmn][3,8]phenanthroline-1,3,6,8-tetraone (NDA-n_0), however, displays a smectic A (S_A) when cooled from the isotropic phase, followed by what appears to be either a highly ordered smectic phase or a columnar phase. This is the first example, known to date, in which a mesophase is detected in a wholly aromatic ether-imide compound. For all compounds we present spectroscopic data and X-ray diffraction data. Cyclic voltammetry was used to determine the redox behavior and pertinent energy levels of the model compounds.

14. SUBJECT TERMS
ether-imide, liquid crystal, organic semiconductor

15. NUMBER OF PAGES
29

16. PRICE CODE
A03

17. SECURITY CLASSIFICATION OF REPORT	18. SECURITY CLASSIFICATION OF THIS PAGE	19. SECURITY CLASSIFICATION OF ABSTRACT	20. LIMITATION OF ABSTRACT
Unclassified	Unclassified		